Journal of Solid State Chemistry **167,** 73–79 (2002)
doi:10.1006/jssc.2002.9621

Influence of Oxygen Nonstoichiometry on the Spectral Properties of Solid Solutions $LaNb_{2-2x}Ta_{2x}VO_{9-\delta}$ ($x = 0$–0.4) and $LaTa_{2-2x}Nb_{2x}VO_{9-\delta}$ ($x = 0$–0.1)

M. G. Zuev,*[,1] E. V. Arkhipova,* L. A. Perelyaeva,* L. V. Zolotukhina,* O. B. Lapina,† and R. N. Pletnev*

*Institute of Solid State Chemistry, Ural Branch of Russian Academy of Sciences, 91 Pervomais kaya. Str., Ekaterinburg GSP-145, 620219 Russia; and †Institute of Catalysis, Siberian Branch of Russian Academy of Sciences, 630090 Novosibirsk, Russia

Received December 6, 2001; in revised form April 5, 2002; accepted April 19, 2002

Phase equilibria in the $LaVO_4$–Nb_2O_5–Ta_2O_5 system were analyzed. New solid solutions $LaTa_{2-2x}Nb_{2x}VO_{9-\delta}$ ($x = 0-0.1$) and $LaNb_{2-2x}Ta_{2x}VO_{9-\delta}$ ($x = 0-0.4$) were detected in this system. The structures of the vanadate–niobate $LaNb_2VO_9$ and vanadate–tantalate $LaTa_2VO_9$ are not known. The structures of the vanadate–tantalate $LaTa_2VO_9$ and $LaTa_2VO_9$-based solid solutions are similar to the structure of $LaTa_7O_{19}$, which refers to the hexagonal crystal system. The influence of the oxygen nonstoichiometry $\delta(x)$ on crystallochemical characteristics and spectral properties of these solid solutions were examined by the X-ray phase analysis, IR and radio spectroscopic methods. A correlation between the nonstoichiometry $\delta(x)$ and the volume of a unit cell $V(x)$ of solid solutions $LaTa_{2-2x}Nb_{2x}VO_{9-\delta}$ was found. The IR spectrum of $LaTa_2VO_{9-\delta}$ transformed in going from $\delta = 0$ to $\delta \neq 0$. Two types of VO_4 tetrahedra were formed in solid solutions $LaNb_{2-2x}Ta_{2x}VO_{9-\delta}$ depending on $\delta(x)$. © 2002 Elsevier Science (USA)

Key Words: **solid solutions; oxygen nonstoichiometry; EPR, NMR, IR; Raman spectra.**

1. INTRODUCTION

The processes of formation of substitutional solid solutions on the cation sublattice in complex oxides have been understood fairly well. At the same time, the problem of formation of solid solutions upon replacement of atoms in the anion sublattice requires a more detailed consideration. In this case, a significant role belongs to various defects of the crystal lattice, which appear during synthesis of crystals. These compounds include solid solutions based on vanadates of rare-earth elements (for example, $ScNb_{2-2x}Ta_{2x}VO_{9-\delta}$ (1)). It is known that vanadium tends to change its charge state in such compounds. Therefore, if samples are synthesized in air, some V^{5+} ions are reduced spontaneously and induce defects in the form of V^{4+} ions, which have a considerable effect on various properties of crystals (2). As is known, vanadium-containing compounds and solid solutions on their basis can be used as luminophors and ceramics with a variable dielectric constant (ε). For example, ε changes from 18×10^3 to 0.2×10^9 when $LaTa_2VO_9$ is heated from 1000°C to 1100°C (3). Therefore, the applied significance of these solid solutions also makes it topical to tackle the aforementioned problem.

The present study deals with the influence of an oxygen nonstoichiometry (δ) on spectral properties of substitutional solid solutions $LaTa_{2-2x}Nb_{2x}VO_{9-\delta}$ ($x = 0$–0.1) and $LaNb_{2-2x}Ta_{2x}VO_{9-\delta}$ ($x = 0$–0.4), which are formed in the $LaVO_4$–Ta_2O_5–Nb_2O_5 system. It is known that Ta^{5+} and Nb^{5+} have similar effective ionic radii at equal coordination numbers (CN). For example, the ionic radii of Ta^{5+} and Nb^{5+} are 0.064 nm (CN = 6) and 0.069 nm (CN = 7), respectively (4). This similarity of the ions suggests a high reliability of their mutual substitution and a minimum distortion of the crystal lattice in the solid solutions. The IR spectrum of $LaTa_2VO_{9-\delta}$ transformed when the nonstoichiometry changed from $\delta = 0$ to $\delta \neq 0$. The transformation was caused by oxygen vacancies in the crystal lattice of this compound. V^{4+} ions formed at $\delta(x) \neq 0$ were located from the EPR spectra. According to the ^{51}V NMR data, two types of VO_4 tetrahedra appeared in solid solutions $LaNb_{2-2x}Ta_{2x}VO_{9-\delta}$ depending on $\delta(x)$.

2. EXPERIMENTAL

The test samples were synthesized by multi-stage annealing of a mixture of starting components in air. The

[1] To whom correspondence should be addressed. Fax: +7-3432-744495. E-mail: zuev@ihim.uran.ru.

0022-4596/02 $35.00

starting components were La_2O_3, Ta_2O_5, Nb_2O_5 and V_2O_5 containing not less than 99.99% of the base material. Stoichiometric quantities of the starting materials were weighed, mixed and ground in an agate mortar under ethyl alcohol. Then the well-mixed powders were placed in corundum boats and were sintered at a temperature between 600°C and 1100 ± 25°C. The mixtures were carefully ground each time the temperature was elevated. The sintering time was 250 h. The phase composition of the samples was determined on a DRON-2.0 diffractometer (Cu$K\alpha$ radiation). The IR spectra were measured on a Specord IR-75 spectrometer in the interval from 1100 to 400 cm^{-1}, while the Raman spectra were obtained on a "Renishaw-1000" spectrometer ($\Delta\nu$ up to 1000 cm^{-1}) using an argon laser ($\lambda = 514.5$ nm) for excitation. The homogeneity interval was determined by the X-ray phase analysis and the IR method. The EPR spectra were recorded on an ERS-220 spectrometer in the X band at room and liquid-nitrogen temperatures.

The ^{51}V NMR measurements were performed on a Bruker MSL-400 spectrometer in a magnetic field of 9.4 T corresponding to a ^{51}V resonance frequency of 105.20 MHz. ^{51}V chemical shifts were referred to external $VOCl_3$. The high-speed MAS ^{51}V NMR spectra were recorded at a rotation frequency of 10–15 kHz using 5-mm (outer diameter) Si_3N_4 rotors and an NMR probe from NMR Rotor Consult. ApS (Denmark). Parameters of the ^{51}V NMR spectra were determined from intensities of the MAS rotational sidebands using the SATRAS approach. Both the ^{51}V static and MAS NMR spectra were simulated taking into account the second-order quadrupole correction using the NMR5 program described elsewhere. All the simulations were performed on a dual PII-400 MHz CPU IBM PC compatible computer running Linux OS.

3. RESULTS AND DISCUSSION

Phase relations of the $LaVO_4$–Ta_2O_5–Nb_2O_5 system in the subsolidus region up to a temperature of 1100°C are shown in Fig. 1. Solid solutions $LaTa_{2-2x}Nb_{2x}VO_{9-\delta}$ ($x = 0$–0.1) and $LaNb_{2-2x}Ta_{2x}VO_{9-\delta}$ ($x = 0$–0.4) were revealed for this system. Two-phase regions are hatched in the diagram. An equilibrium in the three-phase regions (not hatched) was confirmed by an X-ray phase analysis of the samples synthesized in those regions of the system. A mixture of $LaTa_{1.8}Nb_{0.2}VO_{9-\delta}$ and $LaNb_{1.2}Ta_{0.8}VO_{9-\delta}$ phases was detected experimentally in Sections 1 and 2 (see Fig. 1). Figs. 2a and 2b present X-ray diffraction patterns of the synthesized solid solutions. Crystalline structures of $LaTa_2VO_9$ (5) and $LaNb_2VO_9$ (6) are unknown. An X-ray phase analysis showed that the structure of solid solutions $LaTa_{2-2x}Nb_{2x}VO_9$ approached the structure of $LaTa_7O_{19}$, which refers to the hexagonal crystal system. Therefore, it

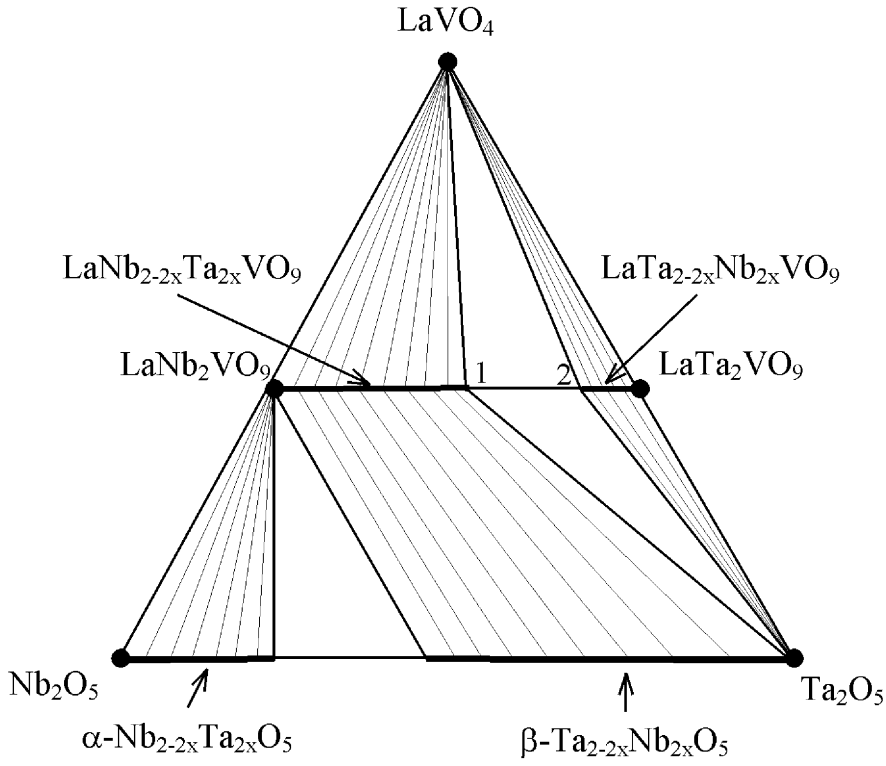

FIG. 1. Subsolidus phase relations in the $LaVO_4$–Nb_2O_5–Ta_2O_5 system.

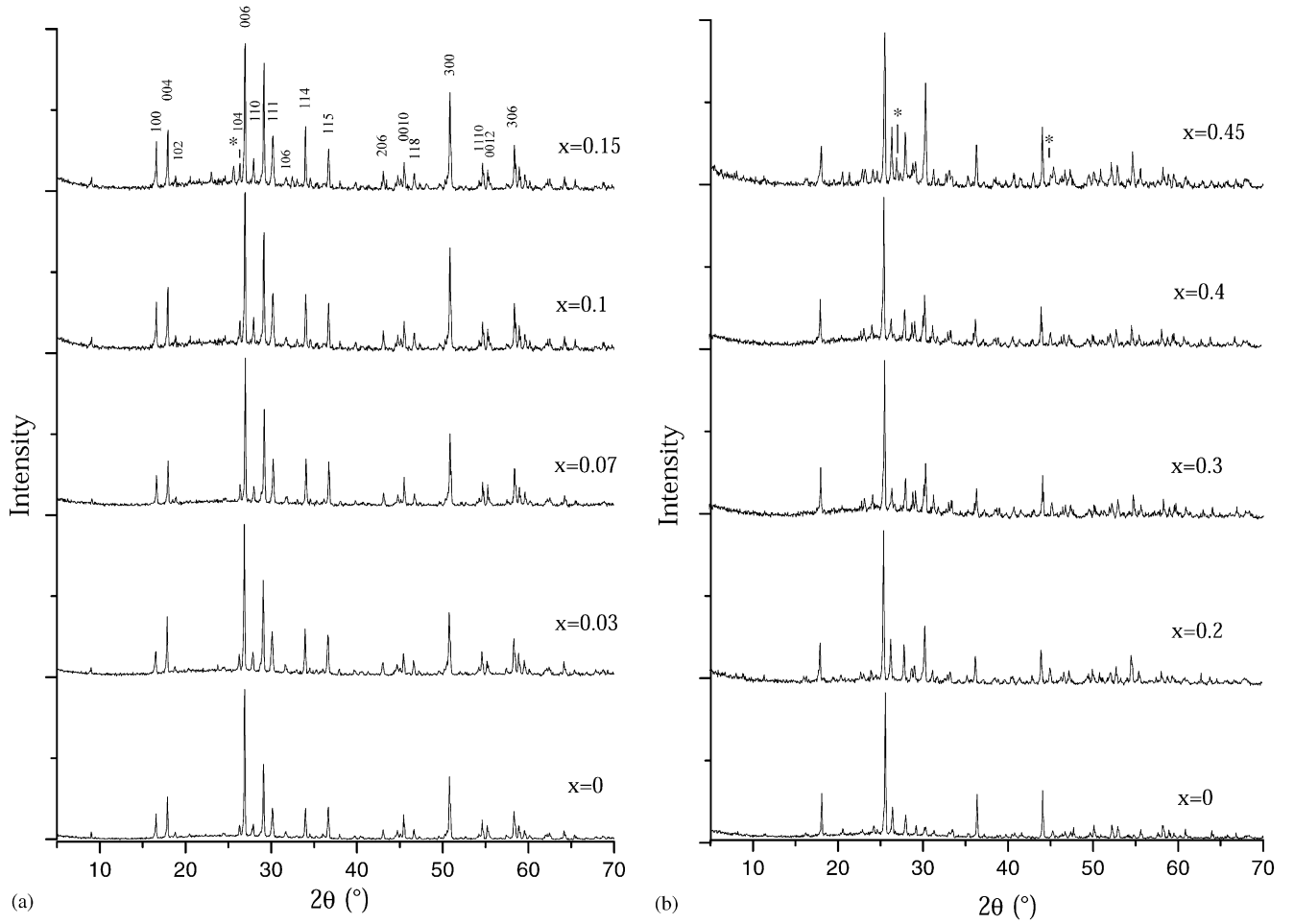

FIG. 2. X-ray diffraction patterns of (a) $LaTa_{2-2x}Nb_{2x}VO_{9-\delta}$ (*is $LaTa_{2-2x}Nb_{2x}VO_{9-\delta}$ ($x=0.1$)). (*is $LaNb_{2-2x}Ta_{2x}VO_{9-\delta}$ ($x=0.4$)) and (b) $LaNb_{2-2x}Ta_{2x}VO_{9-\delta}$

was possible to calculate the crystal lattice parameters of the solid solutions.

EPR signals, whose shape and intensity depended on the phase composition, were detected in all the samples studied. The most intensive signals have the center of gravity corresponding to $g=1.973$. Therefore, they may be related to d^1-electrons of V^{4+}. The appearance of V^{4+} ions is conditioned apparently by an oxygen nonstoichiometry, which arises spontaneously in the samples as a result of solid-state reactions. The oxygen nonstoichiometry (δ) was estimated from the EPR signal. After the $LaTa_2VO_{9-\delta}$ sample was annealed in air at a temperature $\approx 1110°C$ for 8 h, the EPR signal disappeared. This was an indication that the structure of the samples again was complete with respect to oxygen ($\delta = 0$). Figure 3 presents concentration dependences of $\delta(x)$ for solid solutions $LaTa_{2-2x}Nb_{2x}VO_{9-\delta}$ ($x=0$–0.1) and $LaNb_{2-2x}Ta_{2x}VO_{9-\delta}$ ($x=0$–0.4).

Composition dependences of the parameters (calculated to within ± 0.001 Å) and the volume of a unit cell in solid solutions $LaTa_{2-2x}Nb_{2x}VO_{9-\delta}$ are shown in Fig. 4. The dependences $c(x)$ and $V(x)$ exhibit a plane maximum at $x \approx 0.06$. The values of the unit-cell parameters are scattered a little. A similar scatter of the parameter values is known for, e.g., $Nb_{2x}Ta_{2-2x}O_5$ solid solutions. This scatter may be caused, among other things, by appearance of a superstructure (7). Probably, a scatter of the cell parameters is characteristic of oxide solid solutions with mutual substitution of Ta and Nb atoms. The composition dependence of the unit-cell volume in solid solutions $LaTa_{2-2x}Nb_{2x}VO_{9-\delta}$ and the dependence $\delta(x)$ evidently are correlated (Figs. 3a and 4). The function $\delta(x)$ has a minimum at $x \approx 0.05$. When the niobium concentration of these solid solutions increases from 0 to 0.05, δ decreases, i.e., the crystal structure is more complete in oxygen. This leads apparently to an increase in the unit-cell volume of the crystals. If x increases further from 0.05 to 0.1, the number of oxygen defects in the lattice rises. As a result, the volume of a unit cell in the solid solutions diminishes.

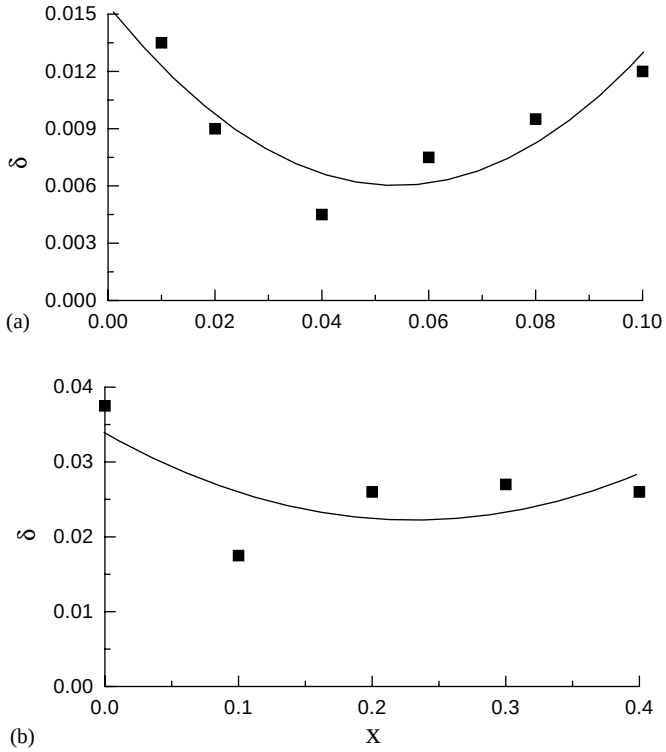

FIG. 3. Concentration dependence of the oxygen nonstoichiometry (δ) of solid solutions $LaTa_{2-2x}Nb_{2x}VO_{9-\delta}$ (a) and $LaNb_{2-2x}Ta_{2x}VO_{9-\delta}$ (b).

The ^{51}V NMR spectra of solid solutions $LaNb_{2-2x}Ta_{2x}VO_{9-\delta}$ contain a line with $\delta_{iso} = -609 - -611$ ppm, whose position does not depend on x within the measurement accuracy. NMR parameters of this line almost coincide with ^{51}V NMR parameters of $LaVO_4$ ($\delta_1 = -555$ ppm, $\delta_2 = -616$ ppm, $\delta_3 = -657$ ppm, $\delta_{iso} = -609$ ppm, $\Delta\delta_{iso} = -100$ ppm; quadrupole constant $C_Q = 5.21$ MHz; asymmetry parameter $\eta_Q = 0.69$ for the quadrupole coupling). The V–O distance varies within 1.693–1.724 Å in $LaVO_4$ (8). Thus, one may assume that vanadium atoms in these solid solutions are located in an isolated nearly regular tetrahedral oxygen environment. When $x = 0$–0.2, an additional line, which corresponds to a less symmetrical environment of vanadium atoms, appears typically. When x increases from 0 to 0.2, the line intensity vanishes monotonically. At the same time, the line with $\delta_{iso} = -610$ ppm widens. The appearance of less symmetric VO_4 tetrahedra in the given range of x probably also depends on the oxygen nonstoichiometry of the solid solutions. Actually, at $x = 0$, the value of nonstoichiometry δ in $LaNb_{2-2x}Ta_{2x}VO_{9-\delta}$ is nearly equal to 0.036. When x varies between 0 and 0.2, the nonstoichiometry δ decreases nearly by a factor of 1.8 (Fig. 3b). The number of oxygen defects in the crystal lattice of the solid solutions drops. Consequently, the number of less symmetric VO_4 tetrahedra decreases too. At $x = 0.2$, tetrahedra of this type disappear. As x increases up to 0.4, only one type of nearly tetrahedral sites of vanadium is left in the structure. The fact that one type of tetrahedra is observed despite an insignificant increase in nonstoichiometry δ may be explained by stabilization of VO_4 in the crystal lattice by the tantalum admixture. Therefore, oxygen defects affect little the formation of VO_4 in the structure of the solid solutions.

The IR spectrum of $LaTa_2VO_9$ ($\delta = 0$) is shown in Fig. 5 (curve 1). When an oxygen nonstoichiometry arises, the IR spectra reflect local distortions in the $LaTa_2VO_{9-\delta}$ structure. The bands shift from 966 to 958 and from 888 to 880 cm^{-1}. New bands 852 and 835 cm^{-1} appear, while the intensity of some bands changes considerably (Fig. 5, curves 2, 3). Moreover, the spectrum from 852 to 770 cm^{-1} in $LaTa_2VO_{9-\delta}$ becomes similar to its counterpart in solid solutions $LaNb_{2-2x}Ta_{2x}VO_{9-\delta}$ with respect to the number, the position and the intensity ratio of the bands (Fig. 5, curves 4 – 6). This may suggest that the crystal lattice of the oxide $LaTa_2VO_{9-\delta}$ and $LaTa_2VO_{9-\delta}$-based solid solutions contains some fragments of the structure of $LaNb_2VO_{9-\delta}$. The stoichiometric $LaTa_2VO_9$ sample was free of such fragments. This microheterogeneous character of solid

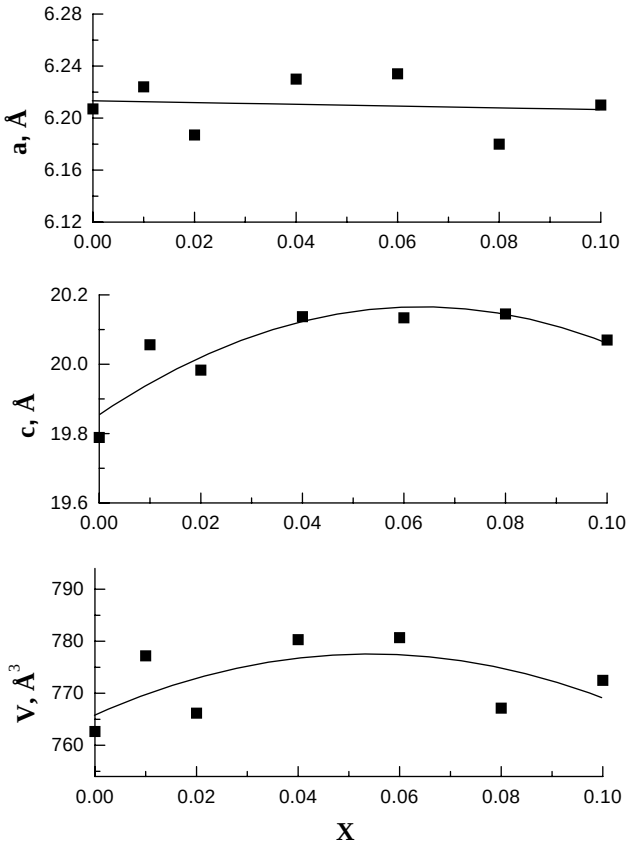

FIG. 4. Concentration dependence of the lattice parameters a and c and the volume V of the solid solution $LaTa_{2-2x}Nb_{2x}VO_{9-\delta}$.

TABLE 1
IR and Raman Frequencies for Solid Solutions $LaTa_{2-2x}Nb2_xVO_{9-\delta}$

$X=0$ ($\delta=0$)	0 ($\delta\neq0$)		0.02		0.04	0.06	0.08		0.1			Assignment
IR	IR	Raman	IR	Raman	IR	IR	IR	Raman	IR	Raman		
		—		—				979		979		
966	958		958		956	958	964		960			
888	880		880		878	880	880		880			
		—		875				878		—		
		851		856				858		855	←	ν_1 VO_4
—	852		852		852	853	852		852		←	Oxygen vacancies
		—		840				842		—		
—	835		835		835	835	836		835		←	Oxygen vacancies
820	821		822		820	822	822		822			
		810		817				820		815		Stretching vibrations
800	802		803		803	804	803		804			of VO_4, TaO_m, NbO_n
		786		790				792		788		
		764		767				769		768		
778	778		778		778	778	778		778			
672	672		672		672	672	672		672			
		661		—				663		663		
618	618		618		616	619	618		620			
		—		—				610		—		
586	586		586		586	586	586		585			
		570		573				573		570		
		541		541				539		538		
520	522		518		522	520	520		520			
		476		—				478		478		
472	472		472		472	472	472		472			
436	436		436		436	436	436		438			
		433		438				440		436		
		397		398				398		396		
		369		373				374		372		
		—		—				359		—		Deformation vibrations
		348		348				348		348		of VO_4, TaO_m, NbO_n
		326		328				327		327		
		309		309				314		310		
		—		—				279		281	←	ν(La–O)
		249		249				249		246		
		225		229				232		232		
		—		204				—		—		
		190		190				192		190		Translation and
		167		167				169		168		rotation of VO_4
		—		147				140		147		
		91		92				93		92		

solutions was observed earlier (9). The new bands at 852 and 835 cm^{-1} may be due to oxygen vacancies. For example, it was shown for an $LaTa_7O_{19}$ crystal, which is isostructural to $LaTa_2VO_9$, that oxygen vacancies located near a lanthanum ion induced quasilocal vibrations at two frequencies in the optical region of the spectrum. The appearance of oxygen vacancies near tantalum atoms does not cause distortions of the vibration spectrum (10). Since an oxygen nonstoichiometry leads to the formation of V^{4+} ions, one may assume that oxygen vacancies are located near vanadium ions in the structure of the solid solutions studied.

The IR spectra of solid solutions $LaTa_{2-2x}Nb_{2x}VO_{9-\delta}$ have an analogous form (Fig. 5, curves 2 and 3). The frequency bands in the 700–970 cm^{-1} range may be related to the region of valence oscillation frequencies of polyhedra VO_4, TaO_m and NbO_n. However, it is difficult to assign all frequencies to oscillations of particular bonds in these complex structures. Therefore, frequencies in the vibration spectra may be assigned just roughly (Tables 1 and 2). Two high-frequency bands at 956–966 and 878–888 cm^{-1} are conditioned by stretching vibrations of Ta–O and Ta–O–La bonds in the lattice of $LaTa_{2-2x}Nb_{2x}VO_{9-\delta}$ (Table 1). Bands caused by deforma-

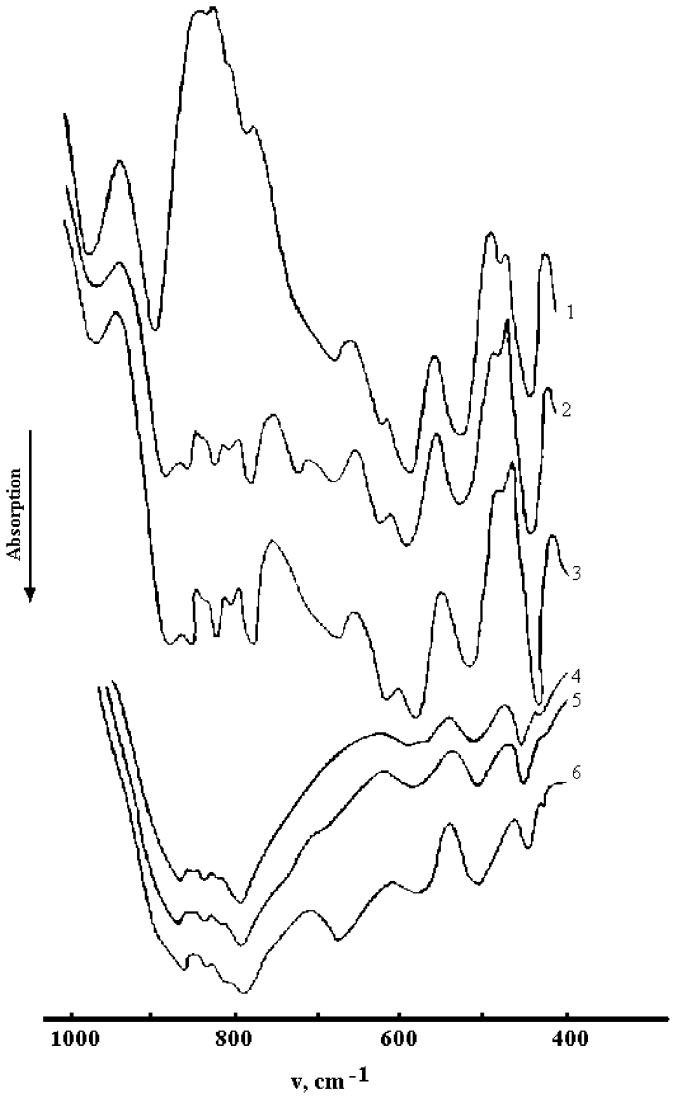

FIG. 5. Infrared absorption spectra: ($\delta = 0$) $x = 0$(1), ($\delta \neq 0$) $x = 0$(2), 0.1(3) for $LaTa_{2-2x}Nb_{2x}VO_{9-\delta}$ and $x = 0$(4), 0.1(5), 0.4(6) for $LaNb_{2-2x}Ta_{2x}VO_{9-\delta}$.

tion vibrations of the said polyhedra and vibrations of La–O bonds are located at frequencies less than 522 cm^{-1}. Some vibrations obviously have a composite nature.

The Raman spectra of solid solutions $LaTa_{2-2x}Nb_{2x}VO_{9-\delta}$ are shown in Fig. 6. All the spectra are similar to one another. A comparison of the frequencies in the IR and Raman spectra of these crystals points to the fulfillment of the exclusion principle. Therefore, when x and $\delta(x)$ change, the crystals remain centrosymmetrical. The most intensive line in the Raman spectra, which may be assigned to the ν_1 vibrations of VO_4 tetrahedra (2), is quite remarkable. This frequency increases continuously from 851 ($x=0$) to 858 cm^{-1} ($x=0.08$). Probably, in the interval of x from 0 to 0.08 the chemical bonds assigned to ν_1 vibrations in VO_4 become shorter. At $x=0.08\rightarrow0.1$ the bond length increases again. The dependence of the chemical bond length on x is correlated generally with the dependence $\delta(x)$ (Fig. 3a) having a minimum at $x\approx0.05$. Probably, when the number of oxygen defects is reduced, VO_4 tetrahedra in the lattice of the said solid solutions are distorted to a lesser extent.

In the interval of x from 0 to 0.4, frequencies in the IR spectra of solid solutions $LaNb_{2-2x}Ta_{2x}VO_{9-\delta}$ drop monotonically from 822 to 818 and from 805 to 800 cm^{-1}. The positions of the other bands in this range of x are fixed. The bands from 800 to 822 cm^{-1} may probably be assigned to the ν_3 vibrations of the VO_4 tetrahedra (Table 2). Therefore, the length of the chemical bond corresponding to this frequency increases monotonically with growing x. The initial structure of the crystals changes insignificantly and, consequently, these solid solutions provide a greater substitution than $LaTa_{2-2x}Nb_{2x}VO_{9-\delta}$. The two types of VO_4 tetrahedra detected in the ^{51}V NMR spectra are not resolved in the IR spectra of these crystals.

So, an oxygen nonstoichiometry of substitutional solid solutions based on ternary oxides affects spectral properties of the solid solutions. IR, EPR and NMR spectra

TABLE 2
IR Frequencies for Solid Solutions $LaNb_{2-2x}Ta_{2x}VO_9$

$X=0$	0.1	0.2	0.3	0.4		Assignment
852	854	852	852	850	←	Oxygen vacancies
836	—	835	836	—	←	Oxygen vacancies
822	822	820	820	818		
805	802	800	800	800		Stretching vibrations of VO_4, NbO_n, TaO_m
778	778	776	778	778		
—	680	668	668	660		
570	575	570	570	560		
495	495	492	492	492		Deformation vibrations of VO_4, NbO_n, TaO_m
437	438	435	435	435		

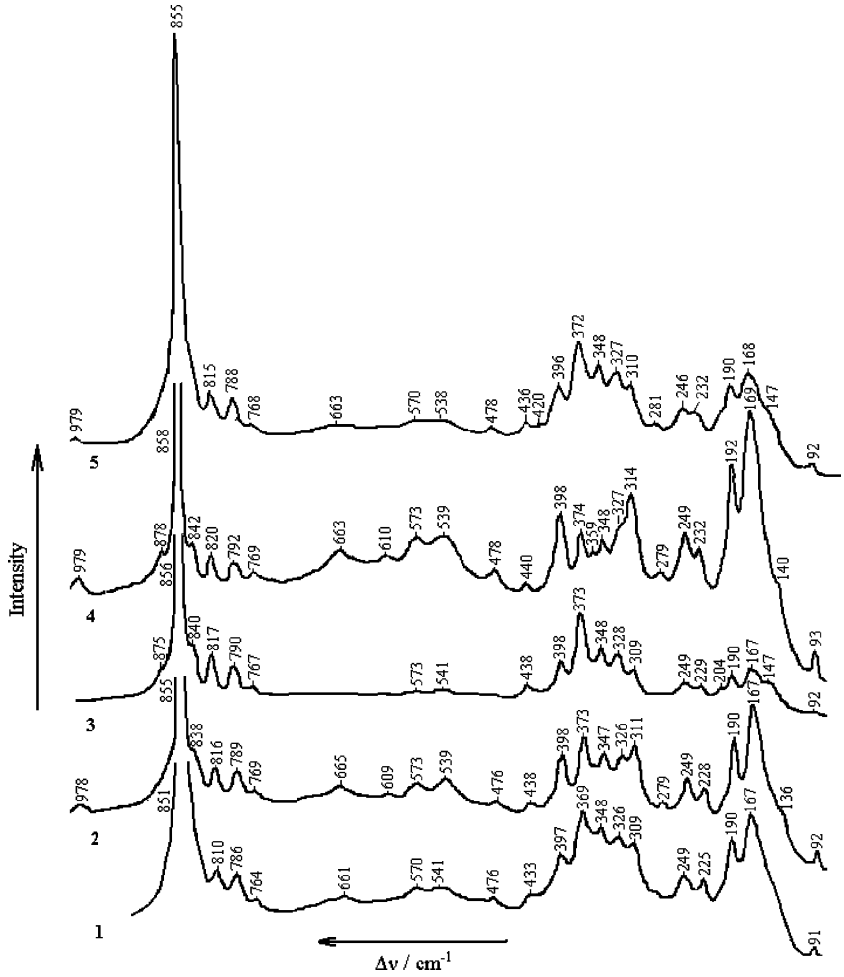

FIG. 6. Raman spectra of solid solutions $LaTa_{2-2x}Nb_{2x}VO_{9-\delta}$: $x = 0(1), 0.01(2), 0.02(3), 0.08(4), 0.1(5)$.

change, reflecting distortions induced in the crystal lattice of the solid solutions by oxygen vacancies.

REFERENCES

1. L. V. Zolotukhina, Ye. V. Zabolotskaya, Ye. V. Arkhipova and M. G. Zuev, *J. Phys. Chem. Solids* **63,** 415–418 (2002).
2. M. G. Zuev, and L. P. Larionov, "Compounds of Rare-Earth Elements with Simple and Complex Anions of the V Subgroup Transition Metals. Synthesis. Compounds. Structure. Properties." Ural Branch RAN, Ekaterinburg, 1999 (in Russian).
3. M. G. Zuev, *Russian Chem. Rev.* **69,** 551–571 (2000), doi: 10.1070/RC2000v069n07ABEN000385.
4. R. D. Shannon, *Acta Crystallogr. A* **32,** 751–767 (1976).
5. Powder Diffraction File. Alphabetical Indexes. Inorganic Phases. Sets 1–47. International Centre for Diffraction Data, Newton Square, PA, 1997. Card No. 40–427.
6. Powder Diffraction File. Alphabetical Indexes. Inorganic Phases. Sets 1–47. International Centre for Diffraction Data, Newton Square, PA, 1997. Card No. 42–107.
7. M. Zafrir, A. Aladjem, and R. Zilber, *J. Solid State Chem.* **18,** 377–380 (1976).
8. C. E. Rice and W. R. Robinson, *Acta Crystallogr. B* **32,** 2232–2233 (1976).
9. A. R. West, "Solid State Chemistry and Its Applications." John Wiley, Sons, New York, 1984.
10. V. G. Mazurenko and M. G. Zuev, *Sov. Phys. Solid State* **34,** 1489–1491 (1992).